XLIII CILAMCE
21–25, November, 2022
FOZ DO IGUAÇU – PR – BRAZIL

On a High-Order Generalized Finite Element Method

André de F. Stabile[1], Sergio P. B. Proença[1]

[1]*Dept. of Structural Engineering, São Carlos School of Engineering, University of São Paulo*
Avenida Trabalhador São Carlense, 400, 13566-590, São Paulo/São Carlos, Brazil
andrestabile@usp.br, persival@sc.usp.br

Abstract. In recent years, technological development has grown exponentially. In this context, numerical methods consist of an attractive tool that guarantees flexibility and ease of access in modeling Science and Engineering problems. In particular, the High-Order version of the Finite Element Method (FEM), based upon orthogonal polynomials as a means for constructing hierarchic approximation spaces, is of special interest, due to its high convergence rate and adequate matrix conditioning. However, albeit FEM achieves good results in a large class of problems, it is not as adequate when non-smooth solutions are expected. Aiming to circumvent such a limitation, the Generalized Finite Element Method (GFEM) introduces enrichment functions, selected on the basis of a previous knowledge about the solution of the problem, in order to enlarge FEM's approximation space. Despite providing scope and generality expansion to the FEM, such technique may lead, nevertheless, to ill-conditioned systems of equations, therefore penalizing numerical precision. Taking this into account, this paper proposes a methodology for integrating positive features of the two aforementioned versions of the FEM, resulting in a stable, precise and high performing numerical tool. The methodology herein presented allows for the possibility of being easily implemented in previously existing codes, already designed to handle GFEM. Planar elasticity applications are considered – including Linear Elastic Fracture Mechanics problems, for which GFEM is more suitable – in order to demonstrate the previously mentioned convergence and conditioning properties of the proposed formulation.

Keywords: GFEM/XFEM, High-Order FEM, Fracture Mechanics, Conditioning, Blending Function Method.

1 Introduction

Numerical methods play a fundamental role in modern engineering analysis. Among those, the Finite Element Method (FEM) is one of the most popular and broadly diffused ones, due to its effectiveness and flexibility when modeling complex domains. It is based off on the construction of a global approximate response as the contribution of many local (and usually polynomial) ones, whose supports are defined on entities called finite elements.

Nevertheless, as every numerical method, it provides only an approximate solution to the mathematical problem at hand. When such solution is not sufficiently accurate it can be refined by means of three main approaches:

- h-refinement, when the size of the elements decrease;
- p-refinement, when the polynomial degree of the local approximations increase; or
- hp-refinement, when both of the above strategies are simultaneously employed.

Even though h-refinements are more widely applied, p and hp strategies achieve, in general, higher convergence rates, as shown in Babuška and Dorr [1] and Babuška et al. [2]. However, depending on their formulation, they can be affected by matrix conditioning problems. To prevent such inconvenience, approximation bases making use of orthogonal polynomials were devised, resulting in a numerically stable version of the FEM that employs p-refinement, called High-Order Finite Element Method (ho-FEM).

However, albeit FEM's versatility in dealing with large classes of problems, it is not as adequate when non-smooth solutions are expected. In this type of situation, the Generalized Finite Element Method (GFEM), which may be understood as an extension of FEM, introduces enrichment functions, selected on basis of a previous knowledge about the solution of the problem, in order to enlarge its approximation space.

Despite providing significant gains of convergence, such technique may lead, nevertheless, to ill-conditioned systems of equations, therefore penalizing numerical precision. Some strategies to prevent this phenomenon are described in the specialized literature, such as modifying the enrichment functions (Babuška and Banerjee [3]) or considering distinct Partitions of Unity (Zhang et al. [4]). However, as exemplified in Sato et al. [5] and Ramos

[6], attaining more than a quadratic convergence rate while simultaneously maintaining good matrix conditioning is not an easy task, even with these techniques.

From the above considerations, the two aforementioned methodologies can be seen as complimentary, in the sense that an union of the two could allow for wider classes of problems than those for which FEM is adequate to be studied whilst preserving numerical stability. Taking this into account, this paper proposes a methodology for integrating positive features of the two of them, resulting in a stable, precise and high performing tool. The methodology is developed in such a way as to allow for the possibility of easy implementation in previously existing codes, already designed to handle GFEM.

In the next sections, a brief exposition of concepts related to ho-FEM and GFEM is given, followed by the formulation of the proposed methodology, called from here on High-Order Generalized Finite Element Method (ho-GFEM). After that, numerical examples are presented – including Linear Elastic Fracture Mechanics problems, for which GFEM is more suitable – in order to demonstrate the previously mentioned convergence and conditioning properties of the formulation. For conciseness, this paper is limited only to planar elasticity problems and the formulation of quadrilateral elements.

2 High-Order Finite Element Method

High-Order versions of the Finite Element Method are based upon the use of orthogonal polynomials as a means of constructing the method's approximation space. Several different bases for such approximation space can be considered. An approach initially conceived was based on employing Legendre polynomials (Szabó and Babuška [7]). In what follows, the basis proposed by Bittencourt [8] is the one chosen to develop the desired methodology. It makes use of Jacobi polynomials, a family of orthogonal solutions of the singular Sturm-Liouville problem, whose expressions can be found on the previously cited book.

2.1 One-dimensional $\mathcal{C}^0$ continuous hierarchical basis

For a one-dimensional finite element on a reference domain $\overline{\Omega} = [-1, 1]$, the following interpolation functions, adequate to represent continuous polynomials up to degree P_1, are employed:

$$\phi_p(\xi_1) = \begin{cases} \frac{1}{2}(1-\xi_1), & p = 0 \\ \frac{1}{2}(1+\xi_1), & p = P_1 \\ \frac{1}{4}(1-\xi_1)(1+\xi_1)P_{p-1}^{\alpha_1,\beta_1}(\xi_1), & 0 < p < P_1. \end{cases} \tag{1}$$

Where $\xi_1 \in [-1, 1]$, the integer index p defines the degree of a specific shape function and $P_{p-1}^{\alpha_1,\beta_1}(\xi_1)$ is a Jacobi polynomial of indexes α_1, β_1 and degree $p-1$.

On eq. (1), the first two expressions correspond to the usual linear Lagrangian shape functions of the FEM, also called vertex modes, while the third one defines shape functions that have support only on interior points of the domain, therefore being referred to as internal modes. The approximation basis above is hierarchical in the sense that for an increasing sequence of polynomial degrees $P_1 < P_2 < \ldots < P_n$ its approximation spaces obey the inclusion relation given by $S_1 \subset S_2 \subset \ldots \subset S_n$.

2.2 Two-dimensional $\mathcal{C}^0$ continuous hierarchical basis for quadrilaterals

The one-dimensional basis given in eq. (1) can be readily extended to a quadrilateral domain $\overline{\Omega}\times\overline{\Omega}$ employing the tensor product operation to generate two-dimensional shape functions:

$$\phi_{pq}(\xi_1, \xi_2) = \phi_p(\xi_1)\phi_q(\xi_2), \quad 0 \le p \le P_1 \;\; e \;\; 0 \le q \le P_2. \tag{2}$$

On the above equation, $\xi_1, \xi_2 \in [-1, 1]$, P_1 and P_2 are the polynomial degrees of approximation on directions corresponding to ξ_1 and ξ_2, and indexes p and q define a specific shape function[1].

This definition induces a classification on the two-dimensional shape functions, which can be either:

- Vertex modes: if both of its generating one-dimensional functions are vertex modes;
- Edge modes: if only one of its generating one-dimensional functions is a vertex mode; or
- Face modes: if both of its generating one-dimensional functions are internal modes.

The specific names on the above classification reflect portions of the quadrilateral domain where the functions have non-zero values, and each one of the three types is illustrated on Fig. 1.

[1] On the expression defining the Jacobi polynomial of shape functions $\phi_q(\xi_2)$, indexes α_1, β_1 should be replaced by α_2, β_2.

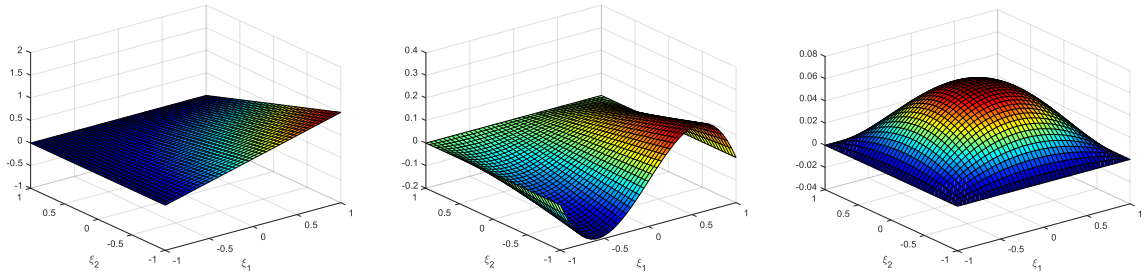

(a) Vertex mode (b) Edge mode (c) Face mode

Figure 1. Different types of High-Order shape functions in two dimensions

2.3 Blending Function Method

On High-Order methodologies the discretization procedure is usually performed by fixing the mesh's element size (usually to a quite large value) and increasing the polynomial degree of approximation. Owing to that, the representation of curved boundaries has an important impact on the quality of results, as they are not approximated by progressively more accurate piecewise polynomials, such as when h-refinement is employed.

An approach to representing in an exact way curved (and possibly non-polynomial) boundaries is the so-called Blending Function Method (BFM) (Gordon and Hall [9]). In this mapping strategy, parametric curves are used to describe the element's boundaries. The geometry interpolation is then given by the usual FEM isoparametric one appended with terms that exactly represent each one of the parametric boundaries on the edge that they refer to and which are then *blended* in such a way that they have no influence on the other edges. Further details, including an instructive example, can be found on Szabó et al. [10].

The following equations describe the mapping:

$$x = \frac{1}{2}\left(\sum_{i=1}^{2}(1+(-1)^i\xi_2)E_{2i-1,x}(\xi_1) + \sum_{i=1}^{2}(1+(-1)^{(i+1)}\xi_1)E_{2i,x}(\xi_2)\right) - \sum_{i=1}^{4}\varphi_i(\xi_1,\xi_2)X_i \tag{3}$$

$$y = \frac{1}{2}\left(\sum_{i=1}^{2}(1+(-1)^i\xi_2)E_{2i-1,y}(\xi_1) + \sum_{i=1}^{2}(1+(-1)^{(i+1)}\xi_1)E_{2i,y}(\xi_2)\right) - \sum_{i=1}^{4}\varphi_i(\xi_1,\xi_2)Y_i \tag{4}$$

Where $E_{i,x}$ and $E_{i,y}$ are the parametric descriptions of coordinates x and y for side i, $\varphi_i(\xi_1,\xi_2)$ are FEM vertex shape functions, X_i and Y_i are node coordinates, and $i = 1,\ldots,4$.

3 Generalized Finite Element Method

The Generalized Finite Element Method's systematic is based upon the idea of augmenting FEM's approximation space by introducing enrichment functions (Sanchez-Rivadeneira and Duarte [11]), which are then made compatible when multiplied by a partition of unity (PoU), usually the Lagrangian FEM vertex shape functions. Conceptually this can be formulated as the partition of the method's approximation space into two other:

$$\mathcal{S}_{GFEM} = \mathcal{S}_{FEM} \oplus \mathcal{S}_{ENR}. \tag{5}$$

With:

$$\mathcal{S}_{FEM} = \left\{\zeta : \zeta = \sum_{\alpha=1}^{N}\phi_{\alpha 0}b_{\alpha 0}; \quad b_{\alpha 0} \in \mathbb{R}\right\}; \quad \mathcal{S}_{ENR} = \left\{\zeta : \zeta = \sum_{\alpha=1}^{N}\sum_{i=1}^{n_\alpha}\phi_{\alpha i}b_{\alpha i}; \quad b_{\alpha i} \in \mathbb{R}\right\}. \tag{6}$$

In the above equations, N is the total number of nodes on the mesh and n_α the number of enrichment functions corresponding to node α. The method's shape functions, $\phi_{\alpha i}$, can be further specialized to (no summation convention implied):

$$\phi_{\alpha i} = \varphi_\alpha \psi_i^\alpha. \tag{7}$$

Where ψ_i^α are the enrichment functions, with $\psi_0^\alpha = 1$.

4 High-Order Generalized Finite Element Method

Following the same ideas behind GFEM, the methodology proposed on this paper partitions its approximation space as the direct sum of other smaller spaces:

$$\begin{aligned} \mathcal{S}_{ho-GFEM} &= \mathcal{S}_{GFEM} \oplus \mathcal{S}_{ho-FEM} \\ &= \mathcal{S}_{FEM} \oplus \mathcal{S}_{ENR} \oplus \mathcal{S}_{EDGE} \oplus \mathcal{S}_{FACE}. \end{aligned} \tag{8}$$

On the above equation, $\mathcal{S}_{ho-FEM}$ was further divided into two spaces corresponding to edge and face modes[2], which can be defined as:

$$\mathcal{S}_{EDGE} = \left\{ \zeta : \zeta = \sum_{\beta=1}^{N_e} \sum_{i=1}^{n_\beta} \phi^e_{\beta i} a_{\beta i} \quad a_{\beta i} \in \mathbb{R} \right\}; \quad \mathcal{S}_{FACE} = \left\{ \zeta : \zeta = \sum_{\gamma=1}^{N_f} \sum_{i=1}^{n_\gamma} \phi^f_{\gamma i} c_{\gamma i} \quad c_{\gamma i} \in \mathbb{R} \right\} \tag{9}$$

where N_e and N_f are the number of edges/faces on the mesh, n_β and n_γ are the number of edge/face modes on a given edge/face, and $\phi^e_{\beta i}$ and $\phi^f_{\gamma i}$ are edge/face functions, given by eq. (2).

The above formulation is conceptually satisfactory as it highlights the possibility of including generic enrichment functions on the proposed methodology, and provides sound mathematical grounds for what is developed. From a practical standpoint, however, a situation in which the High-Order shape functions can be constructed as the product between the PoU and so-called High-Order enrichment functions would be ideal, in order to facilitate integration with pre-existing GFEM codes. Therefore, the design of such enrichment functions is the concern in what follows.

Introducing eq. (1) into eq. (2), a generic local High-Order shape function can be found to have the following form[3]:

$$\phi_{pq}(\xi_1, \xi_2) = \varphi_1(\xi_1)^{m_1} \varphi_2(\xi_1)^{n_1} \varphi_1(\xi_2)^{m_2} \varphi_2(\xi_2)^{n_2} P^{\alpha_1,\beta_1}_{p*}(\xi_1) P^{\alpha_2,\beta_2}_{q*}(\xi_2). \tag{10}$$

Where $m_1, n_1, m_2, n_2 \in \{0, 1\}$ are indexes such that $m_1 + n_1 \geq 1$ e $m_2 + n_2 \geq 1$, $p* = p - 1$ if $0 < p < P_1$ and $p* = 0$ on the contrary. A similar relation is valid for $q*$ replacing P_1 for P_2.

Recognizing that the two-dimensional PoU can be written as a product of the one-dimensional one's components:

$$\varphi_{ij}(\xi_1, \xi_2) = \varphi_i(\xi_1)\varphi_j(\xi_2), \quad 1 \leq i, j \leq 2. \tag{11}$$

Where, for a sequential indexing of nodes of the quadrilateral element starting from the left- and downmost vertex and following a counterclockwise sense, the following association between the indexes i and j and node numbers is valid: $\{11 \to 1,\ 21 \to 2,\ 22 \to 3,\ 12 \to 4\}$.

Equation (11) together with the condition that indexes m_k and n_k ($k \in \{1, 2\}$) do not vanish simultaneously allows for rewriting eq. (10) in the desired format:

$$\phi_{pq}(\xi_1, \xi_2) = \varphi_{ij}(\xi_1, \xi_2)\psi_{pq}(\xi_1, \xi_2). \tag{12}$$

In which $\psi_{pq}(\xi_1, \xi_2)$ collects the remaining terms on eq. (10) and indexes i and j must be chosen according to indexes p and q.

These High-Order enrichment functions, however, cannot be applied on conventional nodes of the finite element mesh. To exemplify the reason for this statement consider node 6 on Fig. 2. If an enrichment function aiming to reproduce a High-Order shape function for edge 6-7 were applied to it, other than appearing on the approximation spaces of elements 2 and 5, as desired, it would also figure on those of elements 1 and 4, where it is not expected.

In order to avoid this problem, High-Order nodes, illustrated on Fig. 3, are introduced. These special nodes do not have a specific PoU pertaining to them, but are rather associated with conventional nodes' PoU components via the relations indicated by the arrows on the figure. Nodes 5 through 8 are responsible for generating edge modes, and each on of them is shared (*i.e.* continuity is imposed) with one adjacent element. Node 9 generates face modes and is not shared with any other element (*i.e.* its shape functions are local).

[2] A third one, referring to vertex modes could have been added here. Nevertheless this is unnecessary, for it would be identical to FEM's approximation space.

[3] On eq. (10) the PoU components are local and one-dimensional. Therefore, $\varphi_i(\xi^j_k) = \delta_{ij}$, with $i, j, k \in \{1, 2\}$ and ξ^j_k being the coordinate of local node j on direction k.

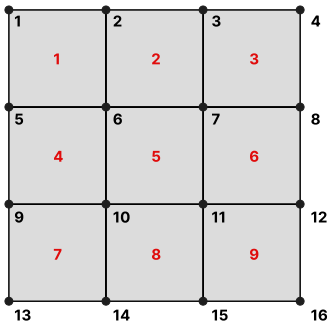

Figure 2. Mesh consisting of 9 finite elements

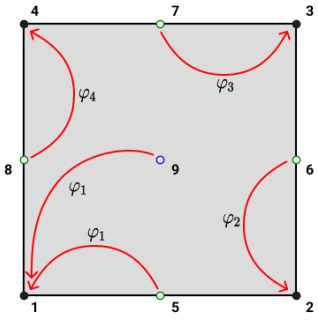

Figure 3. Generalized High-Order finite element

With these concepts, employing eqs. (1) and (2) and the same node numbering as in Fig. (3), the following High-Order edge enrichment functions can be defined:

$$\begin{aligned}
\psi_5^p(\xi_1) &= \varphi_2(\xi_1) P_{p-1}^{\alpha_1,\beta_1}(\xi_1) \quad \Rightarrow \phi_5^p(\xi_1,\xi_2) = \varphi_1(\xi_1,\xi_2)\psi_5^p(\xi_1) \\
\psi_6^q(\xi_2) &= \varphi_2(\xi_2) P_{q-1}^{\alpha_2,\beta_2}(\xi_2) \quad \Rightarrow \phi_6^q(\xi_1,\xi_2) = \varphi_2(\xi_1,\xi_2)\psi_6^q(\xi_2) \\
\psi_7^p(\xi_1) &= \varphi_1(\xi_1) P_{p-1}^{\alpha_1,\beta_1}(\xi_1) \quad \Rightarrow \phi_7^p(\xi_1,\xi_2) = \varphi_3(\xi_1,\xi_2)\psi_7^p(\xi_1) \\
\psi_8^q(\xi_2) &= \varphi_1(\xi_2) P_{q-1}^{\alpha_2,\beta_2}(\xi_2) \quad \Rightarrow \phi_8^q(\xi_1,\xi_2) = \varphi_4(\xi_1,\xi_2)\psi_8^q(\xi_2)
\end{aligned} \tag{13}$$

Analogously, the High-Order face enrichment functions are:

$$\psi_9^{pq}(\xi_1,\xi_2) = \varphi_2(\xi_1)\varphi_2(\xi_2) P_{p-1}^{\alpha_1,\beta_1}(\xi_1) P_{q-1}^{\alpha_2,\beta_2}(\xi_2) \Rightarrow \phi_9^{pq}(\xi_1,\xi_2) = \varphi_1(\xi_1,\xi_2)\psi_9^{pq}(\xi_1,\xi_2) \tag{14}$$

5 Numerical examples

This section is dedicated to showcase two numerical examples on which the developed methodology is applied. The first one is a thick-walled cylinder under internal pressure, having a smooth solution and designed to put the Blending Function Method to test. The second example aims to evaluate ho-GFEM's performance when non-polynomials enrichment are applied, and consists of a panel with an edge crack. Analytic solutions are available to both problems, and the metrics used to evaluate the method's performance are the relative error on the energy norm and the scaled condition number (SCN) of the stiffness matrix (Szabó and Babuška [7]).

5.1 Cylinder with internal pressure

The cylinder's geometry, as well as material properties and boundary conditions, are depicted on Fig. 4. The structure is assumed to behave according to a Plane Stress State. Both h- and p-refinement are tested. In each situation, three meshes with different geometry interpolations, illustrated on Fig. 5, are employed.

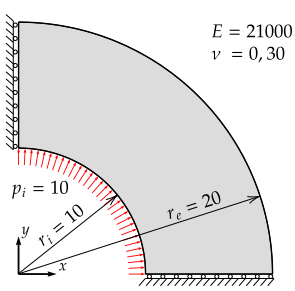

Figure 4. Cylinder

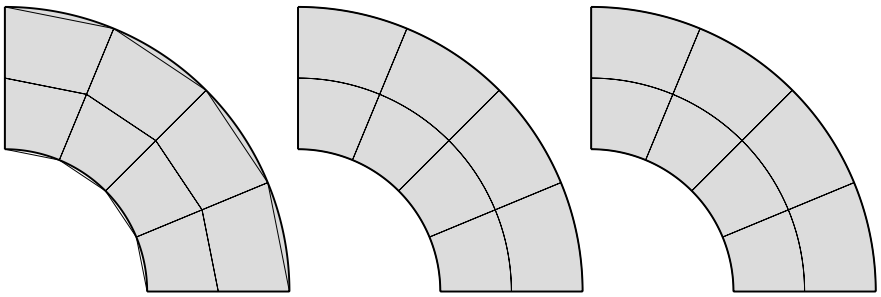

(a) $Q4$ (b) $Q8$ (c) $B4$

Figure 5. Different geometry interpolations

Two of them ($Q4$ and $Q8$) apply the usual linear and quadratic FEM isoparametric interpolations and the other ($B4$) uses the Blending Function Method. The number of elements on straight edges of the cylinder is $2^{(i+1)}$, being the double of this value for curved edges. For h-refinement i goes from 1 to 6 and cases with High-Order enrichments of degrees 1 and 2 are tested, while for p-refinement i is fixed to be 1 and the enrichments'

polynomial degree varies from 0 to 5. An isoparamentric $Q4$ FEM control case is also depicted on some analysis with comparison purposes. Results are summarized on Fig. 6.

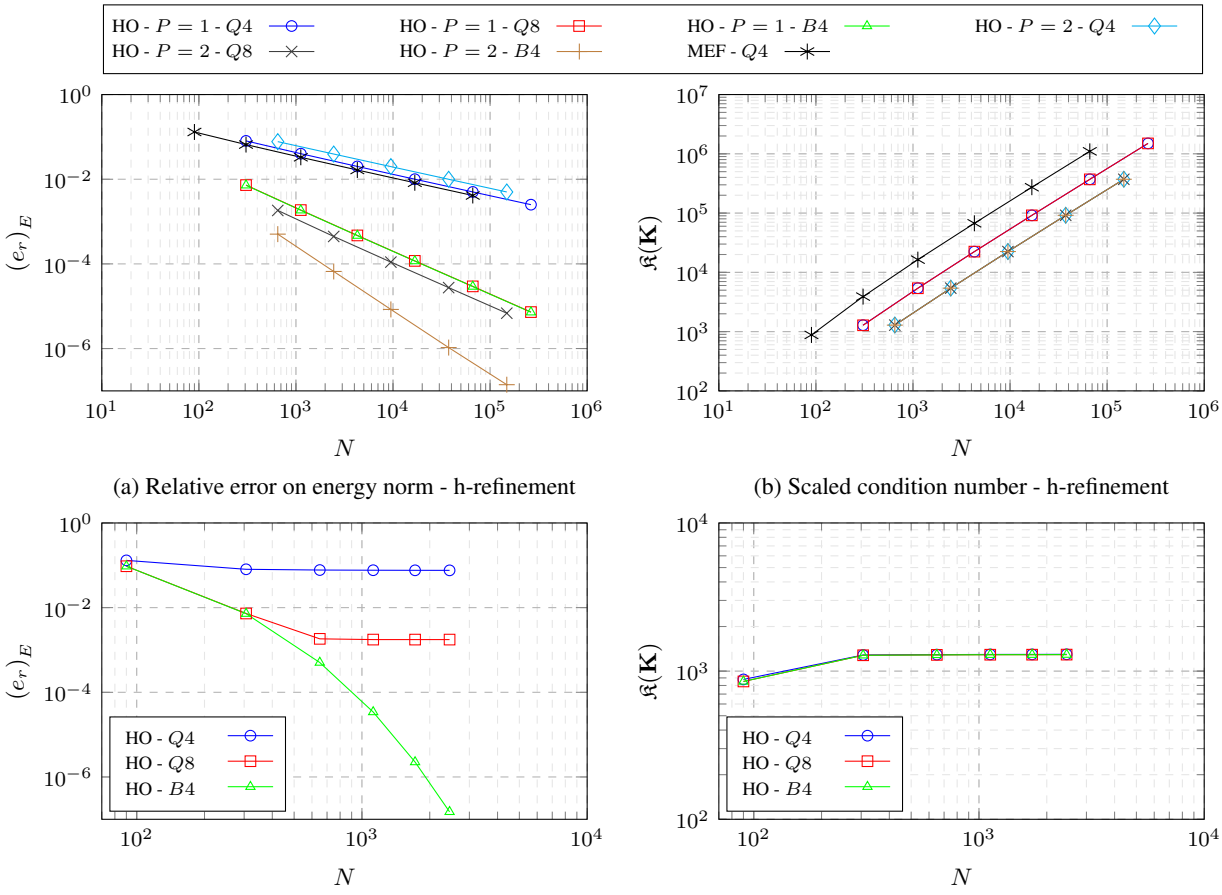

(a) Relative error on energy norm - h-refinement

(b) Scaled condition number - h-refinement

(c) Relative error on the energy norm - p-refinement

(d) Scaled condition number - p-refinement

Figure 6. Cylinder - Relative error on the energy norm and scaled condition number

Figure 6a reveals that even for h-refinement cases the Blending Function Method has an important impact on convergence rates. The plots show that a $Q4$ geometry interpolation bounds the rate of convergence to be $\mathcal{O}(N^{-0.5})$, the same of the FEM, even for cases with linear and quadratic enrichments. A quadratic mapping allows convergence to improve to the expected rate of $\mathcal{O}(N^{-1})$ for a linear enrichment, but impedes its optimal value of $\mathcal{O}(N^{-1.5})$ in the case of a quadratic enrichment. With the BFM, on the other hand, optimal convergence rates are achieved on all cases. Figure 6b reveals that matrix conditioning is unaffected by geometry interpolation, and that the High-Order enrichments preserve the same growth rate of the SCN as in the case of the FEM.

Figure 6c reveals once again, and in a more pronounced way, the importance of the BFM to guarantee convergence. This time, due to the fact that element sizes do not decrease when refinements are performed, the incorrect geometry interpolation not only impairs the convergence rate, but causes the problem's strain energy to converge to an incorrect value. These results are reflected by the plateaus on the $Q4$ and $Q8$ plots. When an exact geometry mapping is applied, conversely, the expected exponential convergence due to p-refinement is achieved. Figure 6d confirms one more time that geometry interpolation has no impact on matrix conditioning and brings to light the excellent stability properties of High-Order enrichments when applied jointly with p-refinement, resulting in an almost constant SCN.

5.2 Panel with edge crack

Figure 7 displays the panel's geometry and material properties. The applied load is self-equilibrated, and corresponds to the first term on the asymptotic expansion of a Mode I loading. Γ_C represents the traction-free edge crack. The problem is assumed to behave in a Plane Strain State. The considered finite element meshes have $2^{(i+1)}$ elements on each side of the panel, and one of them is depicted on Fig. 8. In order to represent the strong discontinuity introduced by the crack, double nodes along its interface were used. High-Order enrichments

are studied together with p- and hp-refinements. For the first one of them, i is fixed to be 1 and the enrichments' polynomial degree varies from 0 to 5, while for the second i equals the polynomial degree of the enrichments and varies from 1 to 4.

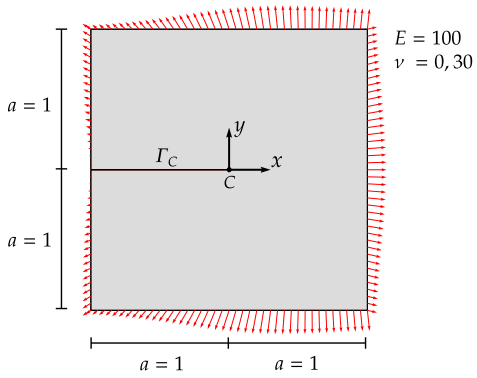

Figure 7. Panel - Geometry

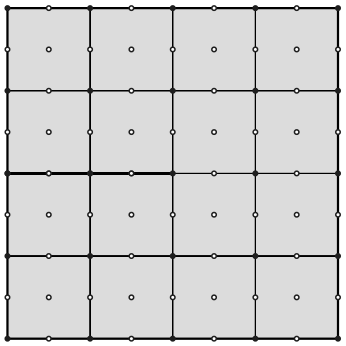

Figure 8. Panel - Mesh

Other than High-Order enrichments, singular ones, also called Oden and Duarte (Oden and Duarte [12]), are also applied. Five cases are studied:

- p-refinement - L_0 w/ HO: whole mesh enriched with HO functions and singular enrichments on L_0;
- p-refinement - L_1 w/ HO: whole mesh enriched with HO functions and singular enrichments on L_1 nodes;
- p-refinement - L_1 w/o HO: L_1 nodes without HO functions, but with singular enrichments;
- hp-refinement - B w/ HO: whole mesh enriched with HO functions and singular enrichments on B nodes;
- hp-refinement - B w/o HO: B without HO functions, but with singular enrichments.

On the above cases, L_0 refers to the crack tip node, L_1 stands for the first layer of elements around L_0 and B denotes the closed ball of radius 0.25 centered at the origin. It is worth to mention that all of the considered cases are instances of a geometric enrichment strategy, which is known to provide good convergence rates (Laborde et al. [13]) when compared with a topological one. Figure 9 depicts the results for this example.

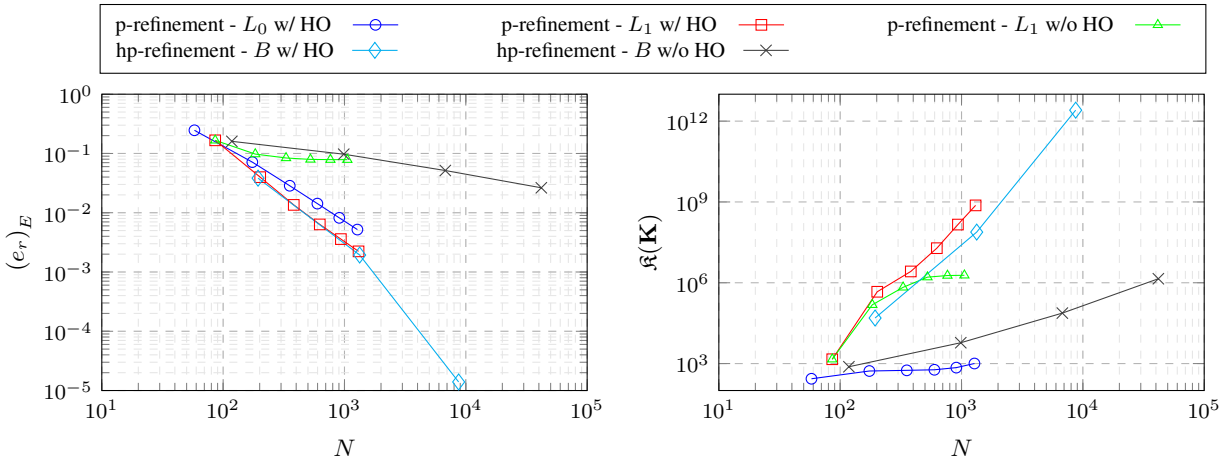

(a) Relative error on the energy norm

(b) Scaled condition number

Figure 9. Panel - Relative error on the energy norm and scaled condition number

Figure 9a shows that the situations for which HO enrichments are not present on the whole mesh did not achieve satisfactory convergence rates: in the case of p-refinement the strain energy almost stagnates, while for hp-refinement the convergence rate is $\mathcal{O}(N^{-0.3})$, only slightly better than that of the FEM.

Other than that, analysis of Fig. 9b highlights that out of the three remaining analysis, those with large areas of interaction between HO and Oden Duarte enrichments exhibit a high rate of growth of the SCN: around $\mathcal{O}(N^5)$ for both p-refinement - L_1 w/ HO and hp-refinement - B w/ HO.

The last case, nevertheless, achieves very good results, with convergence rate of $\mathcal{O}(N^{-1.25})$ and SCN growth of $\mathcal{O}(N^{0.4})$, both of those more than twice as better when compared to the FEM. This can be explained due to the small interaction between HO and singular enrichments, and to the relatively large size of the elements in general, which allows for Oden and Duarte enrichments on the crack tip node to have an important influence area.

6 Conclusions

The numerical problems herein presented demonstrate ho-GFEM's capabilities to produce accurate and numerically stable results. In particular, it is worth to highlight p-refinement's potential to achieve high - and even exponential, when considering smooth problems - convergence rates whilst maintaining the SCN's growth rate to a very low, or even constant, value.

The cylinder example reveals that an exact representation of the problem's geometry, given in the present study by the Blending Function Method, is highly beneficial, not only for p- but also h-refinement problems - context on which the technique is not usually broadly applied.

Other than that, the cracked panel problem demonstrates that the conjoint use of HO and singular functions produces linear dependencies on the method's approximation space. Nonetheless, a judicious choice of the nodes that receive Oden and Duarte enrichments allows these difficulties to be overcome, making it possible to attain a high convergence rate while maintaining good matrix conditioning.

Acknowledgements. The authors would like to thank the Coordenação de Aperfeiçoamento de Pessoal de Nível Superior (CAPES) under process number 88887.600939/2021-00 for the financial support.

Authorship statement. The authors hereby confirm that they are the sole liable persons responsible for the authorship of this work, and that all material that has been herein included as part of the present paper is either the property (and authorship) of the authors, or has the permission of the owners to be included here.

References

[1] I. Babuška and M. R. Dorr. Error estimates for the combined h and p versions of the finite element method. *Numerische Mathematik*, vol. 37, 1981.

[2] I. Babuška, B. A. Szabó, and I. N. Katz. The p-version of the finite element method. *SIAM Journal on Numerical Analysis*, vol. 18, 1981.

[3] I. Babuška and U. Banerjee. Stable generalized finite element method (SGFEM). *Computer Methods in Applied Mechanics and Engineering*, vol. 201-204, pp. 91–111, 2012.

[4] Q. Zhang, U. Banerjee, and I. Babuška. Higher order stable generalized finite element method. *Numerische Mathematik*, vol. 128, pp. 1–29, 2014.

[5] F. M. Sato, D. P. Neto, and S. P. B. Proença. Numerical experiments with the generalized finite element method based on a flat-top partition of unity. *Latin American Journal of Solids and Structures*, vol. 15, 2018.

[6] C. S. Ramos. Partições da unidade flat-top e trigonométricas no método dos elementos finitos generalizados. Master's thesis, Universidade de São Paulo, São Carlos, 2019.

[7] B. A. Szabó and I. Babuška. *Finite Element Analysis*. John Wiley & Sons, Inc., Chichester, 1991.

[8] M. L. Bittencourt. *Computational Solid Mechanics: Variational Formulation and High Order Approximation*. CRC Press, Boca Raton, 2014.

[9] W. J. Gordon and C. A. Hall. Construction of curvilinear co-ordinate systems and applications to mesh generation. *International Journal for Numerical Methods in Engineering*, vol. 7, pp. 461–477, 1973.

[10] B. Szabó, A. Düster, and E. Rank. The p-version of the finite element method. In E. Stein, R. de Borst, and T. J. R. Hughes, eds, *Encyclopedia of Computational Mechanics*, pp. 119–139. John Wiley and Sons, Inc., Chichester, 2004.

[11] A. Sanchez-Rivadeneira and C. Duarte. A stable generalized/extended FEM with discontinuous interpolants for fracture mechanics. *Computer Methods in Applied Mechanics and Engineering*, vol. 345, pp. 876–918, 2019.

[12] J. T. Oden and C. A. Duarte. Clouds, cracks and FEMs. In B. D. Reddy, ed, *Recent Developments in Computational and Applied Mechanics*, pp. 302–321. Barcelona, Spain, 1997.

[13] P. Laborde, J. Pommier, Y. Renard, and M. Salaün. High-order extended finite element method for cracked domains. *International Journal for Numerical Methods in Engineering*, vol. 64, n. 3, pp. 354–381, 2005.